Chemical and Process Engineering 2016, 37 (2), 235-249
DOI: 10.1515/cpe-2016-0019

NUMERICAL MODELLING OF A STOKER FURNACE OPERATED UNDER INDIRECT CO-FIRING OF BIOMASS

Rafał Litka[1,2], Sylwester Kalisz[*1]

[1]Silesian University of Technology, Institute of Power Engineering and Turbomachinery, ul. Konarskiego 20, 44-100 Gliwice, Poland

[2]SBB ENERGY SA, ul. Łowicka 1, 45-324 Opole, Poland

The subject of the CFD analysis presented in this paper is the process of biomass indirect co-firing carried out in a system composed of a stoker-fired furnace coupled with a gasification reactor. The installation is characterised by its compact structure, which makes it possible to minimise heat losses to the environment and enhance the physical enthalpy of the oxidising agent – flue gases – having a favourable chemical composition with oxygen and water vapour. The test results provided tools for modelling of biomass thermal processing using a non-standard oxidiser in the form of flue gases. The obtained models were used to optimise the indirect co-combustion process to reduce emissions. An overall effect of co-combustion of gas from biomass gasification in the stoker furnace is the substantial reduction in NO emissions by about 22%.

Keywords: CFD modelling, stoker, co-firing, gasification, biomass

1. INTRODUCTION

Indirect co-firing usually refers to the gasification of biomass and combustion of the generated gas in the boiler together with its primary fuel. The conversion of biomass into fuel gas makes it possible to avoid some technological problems which arise if the secondary fuel is used for energy purposes in other ways. A novel indirect co-firing concept which utilises flue-gas oxidiser has already been presented elsewhere (Litka and Kalisz, 2012) and the aim of present study is to further analyse the applicability of the novelty through CFD modelling.

The object of the modelling is a stoker-fired water boiler fired with waste from furniture boards - Fig 1. The boiler is equipped with a fire-tube exchanger with the flue gas cross-counter (i.e. two-pass) flow, in which almost entire useful heat is extracted (about 95% of thermal power). A small proportion of the boiler effective power (about 5%) is the heat collected from the cooling of access doors and of the grate. Most of the boiler space is occupied by the furnace, which has no heat transfer surfaces incorporated into the water cycle other than cooled grate bars. The furnace is also a two-pass device. The division of the furnace into the main chamber and the so-called horizontal draft duct improves the combustion quality by lengthening the time of residence of the flue gas combustible fractions in higher temperatures. Moreover, it allows greater flexibility of appropriate distribution of air to individual combustion zones.

The analysed boiler has a furnace with the so-called trough grate. To some extent, the trough grate is a variant of the underfeed stoker because in both solutions fresh fuel is fed under the layer being fired

*Corresponding author, e-mail: sylwester.kalisz@polsl.pl

and the reciprocating motions of the grate bars push the layer farther into the boiler. In the underfeed stoker conventional structures the division into combustion zones, which is typical for commonly used stoker-fired furnaces, does not occur; drying, degassing, gasification and combustion of fuel take place on the almost entire surface area of the grate and the transition from one zone to another occurs in the direction perpendicular to the layer.

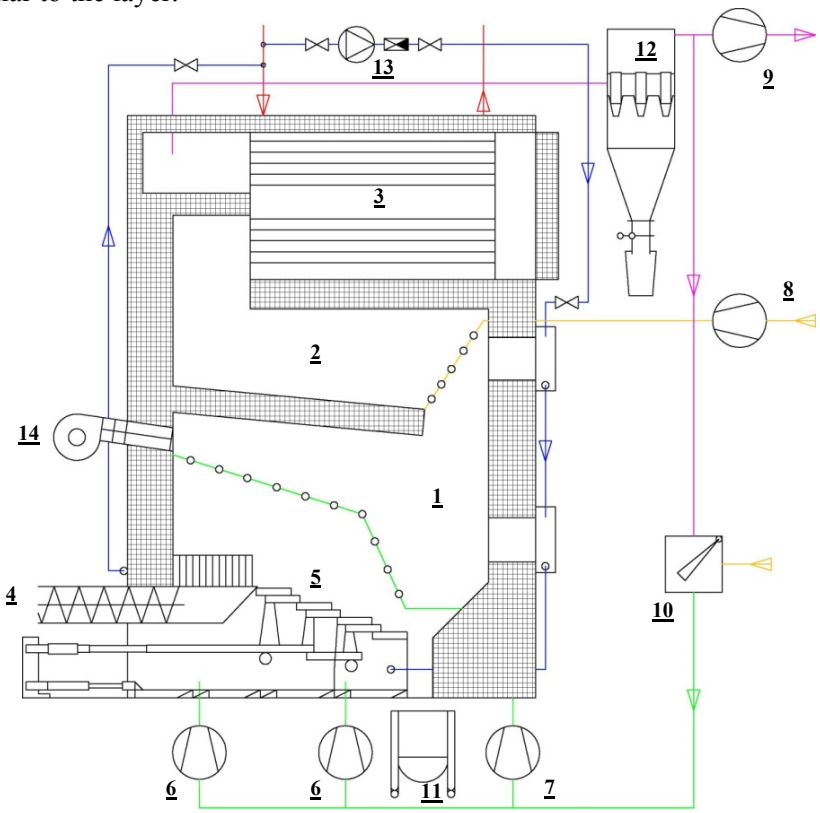

Fig. 1. Boiler flowchart;
1 – main chamber, 2 – horizontal draft duct, 3 – exchanger, 4 – screw feeder, 5 – grate, 6, 7, 8 – primary, secondary and tertiary air fans, 9 – flue gas fan, 10 – recirculation flap, 11 – ash pan, 12 – dust separator, 13 – circulating pump, 14 – light-up burner

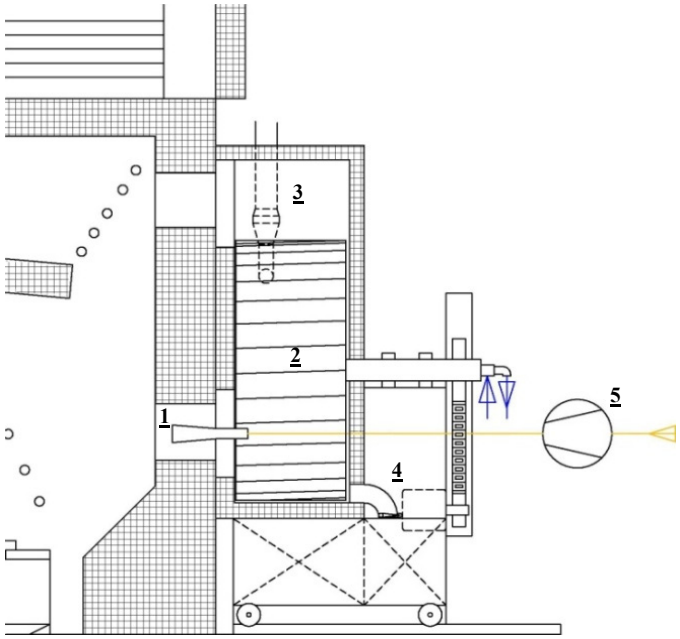

Fig. 2. Gasifier flowchart – integration with the boiler;
1 – jet blower, 2 – rotor, 3 – fuel hopper, 4 – solids discharge, 5 – compressor

The combustion process in a stoker with a trough grate differs significantly from the underfeed stoker – it is much more similar to firing fuel on a travelling grate. In the trough solution the feeder is located below the surface of and at a certain distance from the beginning of the travelling grate. In this way, fuel first fills the space in between the feeder and the grate, creating a layer which is not penetrated by primary air from below. Air (shortage conditions) is only fed into the upper part of the layer through the grate bars which are permanently fixed on the trough edges and its flow is perpendicular to the direction of the fuel path. When the layer level is high enough, degassed fuel spills over onto the first row of moving grate bars from where it is spread over the entire surface of the grate. One consequence of this structure is the furnace fairly strict division into combustion zones: drying and degassing correspond to the buffer area created in between the feeder and the moving grate, coke gasification and combustion take place on the grate and the combustible gaseous products of pyrolysis and gasification are fired on top of the fuel layer and above.

The flue gas-air installation is equipped with five fans with adjustable power: four forced-draught air fans and one induced-draught flue gas fan. The task of each forced-draught fan is to supply the oxidiser to a specific zone of the furnace:

- primary air I – the trough and the first part of the moving grate,
- primary air II – the trough and the second part of the moving grate,
- secondary air (main chamber),
- tertiary air (horizontal draught duct).

Tertiary air is sucked in directly from the boiler room, whereas streams of primary and secondary air, before flowing onto the fans, pass through the space made by the boiler double casing, where they are preheated. Moreover, the connection between the flue gas duct and the channel supplying primary and secondary air allows flue gas recirculation.

A decision was made to improve the boiler effective power using the technology of indirect co-combustion. In this way negative side effects of direct co-combustion are limited (Pronobis et al., 2013). A gasifier was added to the existing boiler (Fig. 2) and the fuel system was modified so that both devices could be fed with the same fuel.

The gasifier structure is based on the rotary furnace solution with a steel rotor and casing. The gasifying medium is sucked into the gasifier through the furnace top access door, whereas the process gas is fed into the main chamber through the bottom access door. The gas flow through the gasifier is forced by a jet blower – operating as the burner at the same time – (Patent PL 212497; Patent PL 212557; Patent PL 214645), for which compressed air is the working medium. Because the ash content in gasified fuel is slight, slag is removed from the gasifier from time to time only.

2. METHODOLOGY

2.1. CFD modelling of the jet blower

The aim of the jet blower modelling was to define the chemical composition and the flow parameters of the air (propelling, working medium) and the process gas (sucked-in medium) mixture at the boiler furnace chamber inlet.

Considering the jet blower geometry, the computational problem was limited to a two-dimensional, axially symmetrical task. The computational area was discretised using a fully structural numerical mesh (Fig. 3) with 16044 elements. The area was composed of four basic sub-areas (in parentheses, respectively: the average, minimum and maximum values of the characteristic dimension of the cell: the square root of the cell surface area):

- working nozzle (~1.63 mm, ~1.18 mm, ~1.80 mm),
- sucking-in chamber (~2.44 mm, ~1.20 mm, ~4.33 mm),
- mixing chamber with diffusor (~2.90 mm, ~1.87 mm, ~7.34 mm),
- furnace (~16.15 mm, ~7.40 mm, ~33.05 mm).

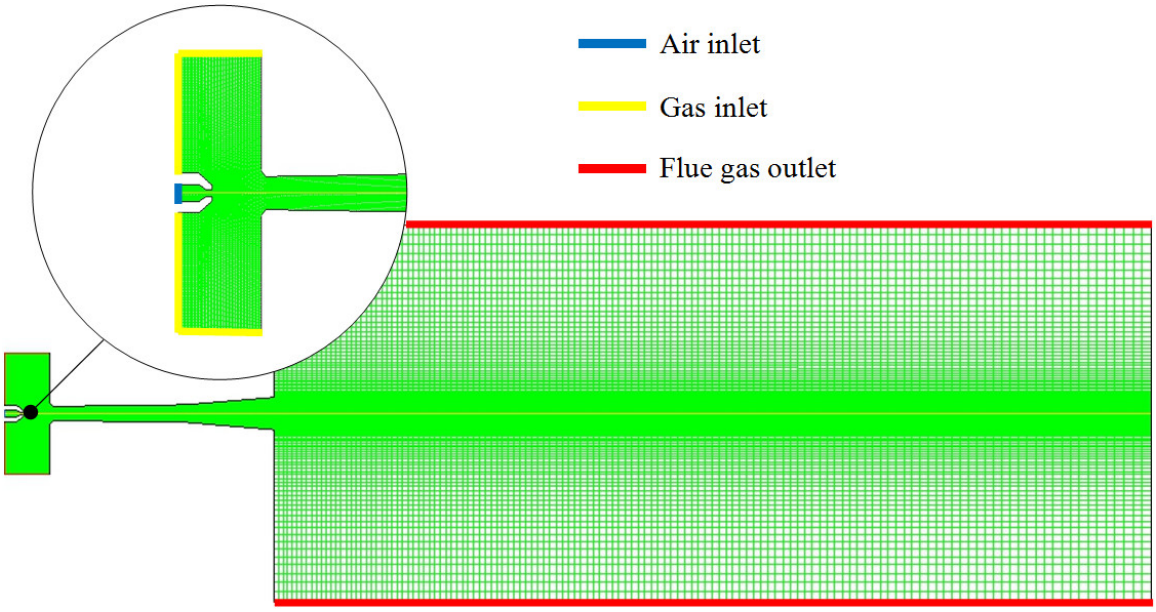

Fig. 3. Numerical mesh for flow modelling in the jet blower

Only the mixing chamber and the diffusor geometries were completely modelled. The dimensions of the model furnace were assumed as the lengths and widths of the boiler main chamber and the dimensions of the sucking-in chamber and the working nozzle were spatially limited to the area having a substantial impact on the flow. The size of a real furnace was taken into consideration to assess the gas spread in the boiler main chamber, which allowed a preliminary evaluation of the correctness of the jet blower parameters selection.

The gasification temperature established based on equilibrium-balance calculations (Litka et al., 2012) was determined taking account of two kinds of losses: the dissipation loss and the heat loss in slag. It is assumed that there is no heat exchange between the boiler and the gasifier through their structural elements. Therefore, on the gasifier side heat flows between the jet blower structure and the inside of the gasifier, whereas on the boiler side – between the jet blower structure and the inside of the main chamber. Undoubtedly, the heat transfer between the jet blower and its immediate surroundings has an effect on the transfer of mass, momentum and energy inside the boiler and gasifier, but it does not affect the energy flux between the devices. Based on that, the modelling was simplified by omitting the heat transfer on the jet blower walls. The heat transfer in the furnace chamber was also omitted because the most interesting flow area, considering the further process of calculations, is the jet blower outlet cross section, the furnace area being modelled for informative purposes only.

The following material properties are determined for the modelled flow:

- The specific heat capacity of all chemical compounds taken into consideration in the flow is a polynomial function of temperature with coefficients determined for two ranges.
- The mixture of the gaseous compounds is a compressible perfect gas with thermal properties (specific heat capacity, heat conductivity, kinematic viscosity) established based on weighted properties of its individual components.
- The gaseous mixture is treated as a grey gas with zero reflexivity (no dispersed phase).

The absence of the dispersed phase in the gaseous mixture is assumed based on previous analyses concerning the need to maintain the highest possible degree of slag bonding in the gasifier and on the

assumption that the transported gas temperature renders the precipitation of tars in the jet blower impossible. Moreover, gasification in conditions ensuring complete conversion of carbon should result in no soot particles in sucked-in gas.

The assumption that there is no dispersed phase and no heat transfer between the gaseous phase and the environment makes it possible to omit the impact of radiation in the modelled flow. What is taken into account, though, is the impact of turbulence and the effect of diffusion.

The two-equation k-ε turbulence model is used, which is common in combustion modelling. Of three versions of the k-ε model available in the FLUENT software package, the realizable model was selected, due to the relatively high pressure gradients characterising the flow in the jet blower (Fluent 6.3 User's Guide, 2006).

The chemical model was developed based on the mechanisms used in the area of biomass thermal processing calculations (de Souza et al., 1989 Dryer et al., 1973; Miltner et al., 2006; Smoot et al., 1985). It is assumed that the reaction rate in the modelled flow depends both on the turbulent effect and on the chemical kinetics defined by the Arrhenius law. Table 1 presents reactions considered in the chemical model (homogeneous reactions 1-8 are used in the jet blower modelling) together with their kinetic equations and the values of kinetic constants.

2.2. CFD modelling of stoker furnace

Because of the furnace geometry complex structure, the geometrical model is divided into 64 sub-areas which, when discretised, make up a single numerical mesh – Fig. 4. The computational area was discretised using both structural and non-structural elements (371,838 and 391,809, respectively). The non-structural elements constitute about 11.5 % of the geometrical model volume. The respective average, minimum and maximum values of the cell characteristic dimension (i.e. cube root of the cell averaged volume) are as follows: ~23.9 mm, ~7.8 mm, ~29.8 mm for structural elements and ~11.9 mm, ~1.6 mm, ~26.4 mm – for non-structural ones.

The furnace geometry is modelled quite precisely. Only the bevelling of some metal elements and the gaps between the permanent elements of the trough grate through which primary air flows are omitted. The gaps between the grate bars are not modelled because their geometry is unknown. The flue gas duct connecting the horizontal draft duct to the exchanger and the flue gas extraction duct connecting the boiler to the gasifier are finished with a surface perpendicular to the duct cross section at a short distance from the furnace because the exchanger and the gasifier areas do not have a significant impact on the analysed combustion quality. The slag discharge channel is limited in the same manner.

The amount of heat carried away from the furnace through the brickwork is found based on the dissipation loss. In modelling the reference state of the boiler (no integration with a gasifier) the computational area surfaces in the furnace top and bottom access doors are taken into account in the heat transfer to the environment, whereas in modelling the upgraded installation – the same surfaces are assumed as adiabatic ones. No heat transfer to the environment is assumed also in the cross section of the biomass feeder outlet.

Stoker boiler modelling is a complex task (Hernik, 2014). Two approaches are common in modelling stoker-fired furnaces using CFD software:

- CFD modelling of combustion in the gaseous phase using boundary conditions determined on top of the burning layer (the boundary conditions on the borders of the computational areas are found using separate software),
- CFD modelling of combustion in the gaseous phase combined with CFD modelling of combustion in a porous bed (single software possible).

Table 1. Kinetic parameters used in CFD modelling of combustion (de Souza et al., 1989; Dryer et al., 1973; Mehrabian et al., 2012; Miltner et al., 2006; Smoot et al., 1985)

Reaction No.	Stoichiometric equation	Kinetic equation r, [kmol/(m^3·s)]	Arrhenius equation coefficients	
			A_r s^{-1}	$E_r/(MR)$ [K]
1	$CH_4 + 1.5O_2 \rightarrow CO + 2H_2O$	$r_1 = k_1 (C_{CH4})^{0.7} (C_{O2})^{0.8}$	1.585×10^{10}	24157
2	$H_2 + 0.5O_2 \rightarrow H_2O$	$r_2 = k_2 (C_{H2})^{1.5} (C_{O2})$	$5.159\times10^{16}\cdot T^{-1.5}$	3420
3	$CO + 0.5O_2 \rightarrow CO_2$	$r_3 = k_3 (C_{CO})(C_{O2})^{0.25} (C_{H2O})^{0.5}$	$3\times25\cdot10^{7}$	20446.3
4	$CO + H_2O \rightarrow CO_2 + H_2$	$r_4 = k_4 (C_{CO})(C_{H2O})$	2.78	1510
5	$NH_3 + O_2 \rightarrow NO + H_2O + 0.5H_2$	$r_5 = k_5 (C_{NH3})(C_{O2})^{0.5} (C_{H2})^{0.5}$	$1.21\times10^{5}\cdot T^{2}$	8000
6	$NH_3 + NO \rightarrow N_2 + H_2O + 0.5H_2$	$r_6 = k_6 (C_{NH3})(C_{NO})$	$8.73\times10^{14}\cdot T^{-1}$	8000
7	$HCN + O_2 \rightarrow NO + CO + 0.5H_2$	$r_7 = k_7 (C_{HCN})(C_{O2})$	10^{10}	33712
8	$HCN + NO \rightarrow N_2 + CO + 0.5H_2$	$r_8 = k_8 (C_{HCN})(C_{NO})$	3×10^{12}	30188
9	$C_{3.878}H_{6.426}O_{3.561} + 0.1585\,O_2 \rightarrow 3.878\,CO + 3.213\,H_2$	$r_9 = k_9 (C_{C3.878H6.426O3.561})^{0.5} (C_{O2})$	$p^{0.3}\cdot5.98\times10^{4}\cdot T$	12200
10	$C + CO_2 \rightarrow 2CO$	$r_{10} = \frac{1}{k_{10}^{-1} + D_{10}^{-1}} (C_{CO2}^{m})$ [kg/(m^2·s]	$3.42\cdot T$ [m/s]	15600
11	$C + H_2O \rightarrow CO + H_2$	$r_{11} = \frac{1}{k_{11}^{-1} + D_{11}^{-1}} (C_{H2O}^{m})$ [kg/(m^2·s]	$3.42\cdot T$ [m/s]	15600
12	$C + 0.5O_2 \rightarrow CO$	$r_{12} = \frac{1}{k_{12}^{-1} + D_{12}^{-1}} (C_{O2}^{m})$ [kg/(m^2·s]	$1.715\cdot T$ [m/s]	9000

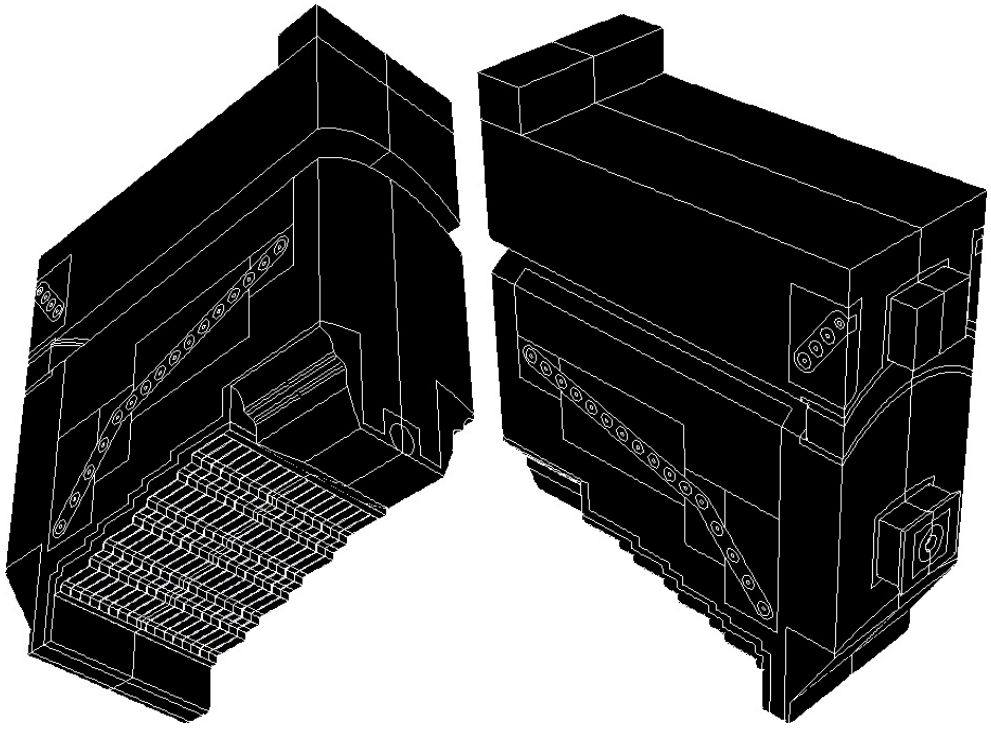

Fig. 4. Geometrical model of the boiler furnace

A simplified method was developed for the purposes of this analysis, which reduces the computational problem to a single-stage CFD modelling of combustion using the dispersed phase model. This approach is based on the following assumptions:

- The furnace model geometry takes account of the area comprising the fuel layer.
- The layer is divided into three zones:
  1. the zone of moisture evaporation and the volatile fraction release (pyrolysis zone),
  2. the zone of coke gasification,
  3. the zone of slag cooling.
- Moisture, volatile fractions and fixed carbon are introduced into the computational area separately: moisture – through the feeder outlet, volatile fractions – through the through bottom and fixed carbon – through the moving part of the grate.
- The ash effect on the combustion process is taken into consideration only in the furnace overall heat balance and in the flue gas properties related to radiation.
- The border between the pyrolysis and gasification zones is located where the layer starts to be penetrated by primary air from below.
- The motion of the grate bars ensures that about 95% of the moving part of the grate are covered with coke (the gasification zone) and the other 5% of the surface remain uncovered (the cooling zone).
- Coke is uniformly oxidised as the layer moves along the grate and its reactivity in the direction transverse to the layer path depends on the concentration of oxygen in the surrounding gaseous atmosphere.
- The resistance of the primary air flow through the layer is independent of the layer height.
- The layer does not conduct heat and its temperature is homogeneous.
- Fixed carbon is fed into the furnace in the temperature of the layer.
- 55% of combustion heat are released on the grate and the remaining 45% – above it (Mikulski, 1954).
- Moisture and volatile fractions are fed into the furnace in the temperature of the surroundings.

In the proposed model, the "layer" is a conventional term related to the fuel substance introduced into the computational area through the grate.

2.3. Input data – modelling assumptions

The calculations were performed for two states:

- the boiler operation with no gasifying reactor – reference state,
- the boiler operation with an installed gasifying reactor – post-upgrade state.

An essential problem in CFD modelling is the selection of an appropriate distribution of air supplied into individual combustion zones. As no measurement data were available, the distribution was made arbitrarily, mapping the operation of a boiler with a trough grate.

The air velocity in the grate gaps should not be smaller than 2-5 m/s for forced circulation boilers (Mikulski, 1954; Ostrowski et al., 1956; Türschmid, 1988). Considering the fuel degassing in the buffer area, it is assumed that the excess air factor on the grate is not required to be very high. On the other hand, the higher velocity (consequently – the greater amount) of air supplied under the grate may cause the fuel particles to be carried away and even result in a loss of the layer stability on the grate (Mikulski, 1954). The flue gas temperature at the furnace chamber outlet should not be lower than 900-1000 °C to prevent losses related to imperfect and incomplete combustion (UBC losses) (Türschmid, 1988). The demand for combustion air is thus a sum of the very non-uniform demand for air needed to fire hydrocarbons and the uniform demand for air to fire coke (Mikulski, 1954).

The maximum amount of secondary air in stoker-fired furnaces is assumed as half the used excess air, i.e. if the excess air factor is 1.5, 25% of the theoretically needed air amount may be supplied as secondary air (Mikulski, 1954). The flowing air relative velocity in relation to the floating fuel particles should be as high as possible to complete the process (gasification and combustion) in the possibly shortest time. For fuels with a very large content of volatile fractions, injection of additional air, referred to as secondary air, may prove necessary not only to mix flue gases but also to supply air to unburnt products of gasification. The screw feeder supplies fuel into the trough, whose rectangular edges are formed by the grate bars that air flows through (Hernik, 2014).

The maximum excess air factor in the main chamber is assumed at the level of 50% (λ = 1.5) because at a higher value the flame cools too fast, which involves higher PAH emissions and a rise in combustible fractions in gaseous and solid products of combustion (joint publication edited by W. Kordylewski (2008)). The flue gas temperature at the furnace outlet is assumed by 50 °C lower than the ash softening temperature (Table 2), i.e. 1150 °C.

Table 2. Characteristic temperatures of fusibility of ash from furniture board waste (according to standard PN-82/G-04535)

	Type of atmosphere	
	oxidising	reducing
sintering temperature	1100 ± 15 °C	1080 ± 16 °C
softening temperature	1200 ± 11 °C	1190 ±16 °C
melting temperature	1210 ± 14 °C	1220 ± 26 °C
flow temperature	1250 ± 16 °C	1240 ± 22 °C

3. MODELLING RESULTS

3.1. CFD modelling of the jet blower

Table 3 shows results of the jet blower system numerical modelling. The presented values were obtained for air with the temperature of 7.5 °C as the assumed propellant. The air pressure was selected to obtain the assumed sucked-in gas mass flow at the inlet of 0.055 kg/s. The maximum velocity obtained at the nozzle outlet was 310.9 m/s, which means that it was higher than the speed of sound (*Ma* > 1). The propellant temperature is 7.5 °C so, expanding locally, the air reaches a static temperature of -39.8 °C.

Table 3. Kinetic parameters of the flow and the maximum and minimum temperatures obtained for the entire modelling area

Quantity	Symbol	Value
Process gas mass flow	$\dot{m}_g$	0.0567 kg/s
Propelling air mass flow	$\dot{m}_p$	0.0457 kg/s
Ejection ratio	$\dot{m}_g / \dot{m}_p$	1.24
Maximum temperature (static)	t_{max}	1901.0°C
Minimum temperature (static)	t_{min}	-39.8°C
Obtained maximum velocity	v_{max}	310.9 m/s

Table 4 presents parameters obtained at the jet blower outlet (the boiler inlet): the flow temperature and velocity and the volumetric composition of the gasification gas and propelling air mixture obtained during the flow through the jet blower. Mixing the gas with a high content of CO with air from the jet blower nozzle results in combustion of combustible gases, which involves a high temperature of the gas leaving the jet blower (up to 1656.8°C maximum). The gas velocity obtained at the jet blower outlet is high – at the level of 58.3 m/s, which ensures appropriate mixing of the gas from the jet blower with the products of combustion in the boiler furnace chamber. Due to the low content of oxygen, another favourable effect is the small amount of NO in flue gases.

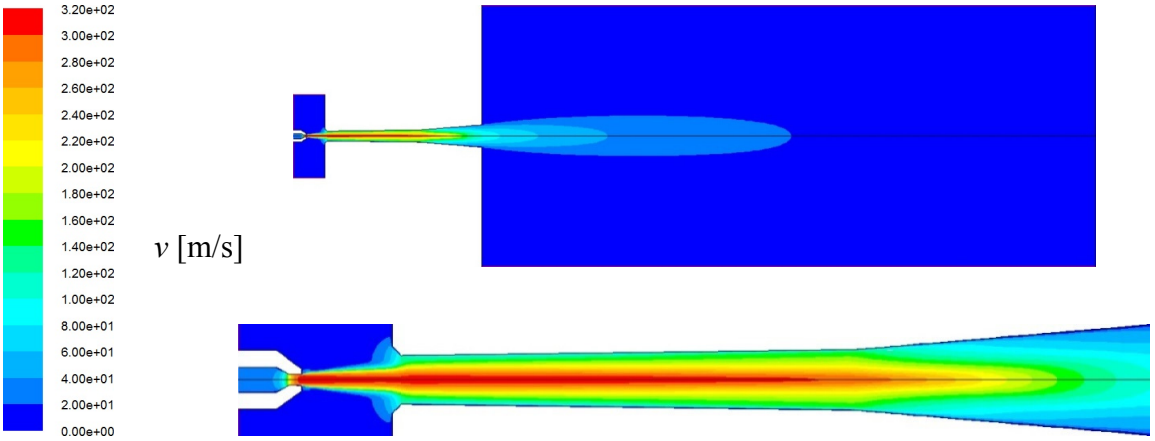

Fig. 5. Velocity fields in the axial section of the entire computational area (top) and of the jet blower area (bottom)

The obtained velocity fields [m/s] in the axial section of the entire computational area and of the jet blower area are presented in Fig. 5. The fields of temperature [K] and of the CO, O_2 and NO molar contents in the axial section of the jet blower area are presented in Fig. 6 and in Table 4.

Table 4. Values obtained in the jet blower outlet cross section (thermal parameters and the gas volumetric composition)

t	*v*	(H_2O)	(N_2)	(CH_4)	(H_2)	(CO)	(CO_2)	(O_2)	(NO)
1656.8 °C	58.3 m/s	12.05%	62.74%	0.47%	4.09%	5.16%	15.44%	0.05%	4 ppm

3.2. CFD modelling of the boiler furnace

Table 5presents results of CFD modelling for the boiler in the reference state and in the post-upgrade state. The table includes the flue gas temperature (*t*) and velocity (*v*) and the CO, O_2 and NO molar contents in flue gases, as well as NO emissions per unit in characteristic points of the modelled area.

Table 5. Results of the boiler furnace modelling

	Furnace outlet		Furnace upper window (flue gas collection)	
	Reference state	Post-upgrade state	Reference state	Post-upgrade state
t	1126.8 °C	1059.9 °C	1153.7 °C	1059.3 °C
v	4.61 m/s	6.83 m/s	4.33 m/s	8.92 m/s
(CO)	< 1 ppm	< 1 ppm	49 ppm	< 1 ppm
(O_2)	7.92%	9.47%	6.01%	8.44%
(NO)	606 ppm	474 ppm (22% reduction)	776 ppm	408 ppm

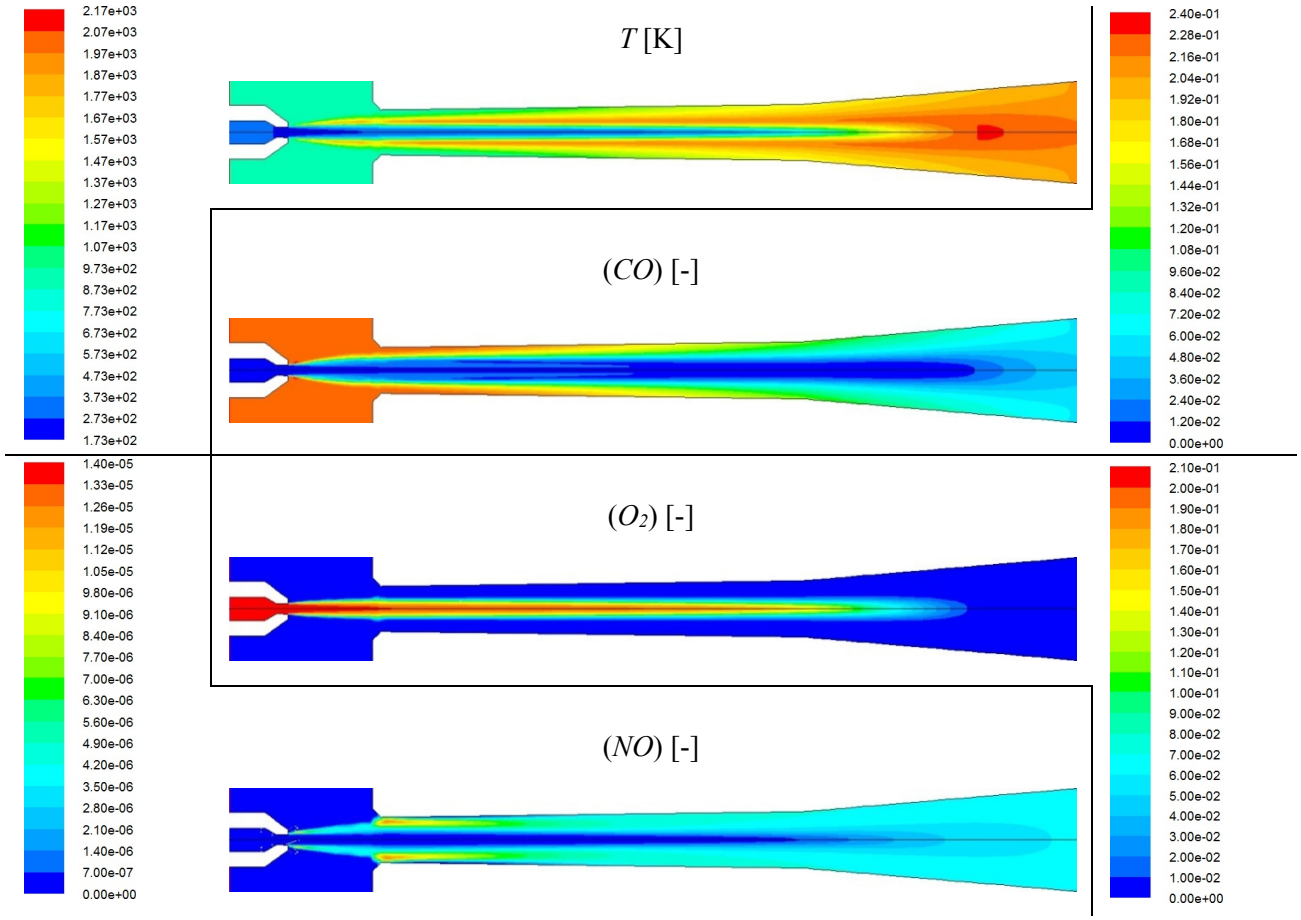

Fig. 6. Fields of temperature [K] and of the CO, O_2 and NO molar contents [-] in the axial section of the jet blower area

3.3. CFD modelling of the boiler furnace

Table 5 presents results of CFD modelling for the boiler in the reference state and in the post-upgrade state. The table includes the flue gas temperature (t) and velocity (v) and the CO, O_2 and NO molar contents in flue gases, as well as NO emissions per unit in characteristic points of the modelled area.

Table 5. Results of the boiler furnace modelling

	Furnace outlet		Furnace upper window (flue gas collection)	
	Reference state	Post-upgrade state	Reference state	Post-upgrade state
t	1126.8 °C	1059.9 °C	1153.7 °C	1059.3 °C
v	4.61 m/s	6.83 m/s	4.33 m/s	8.92 m/s
(CO)	< 1 ppm	< 1 ppm	49 ppm	< 1 ppm
(O_2)	7.92%	9.47%	6.01%	8.44%
(NO)	606 ppm	474 ppm (22% reduction)	776 ppm	408 ppm

The maximum temperature of flue gases in the furnace for the reference state was 2122.7 °C, and the maximum temperature of the furnace walls – 1141 °C. For the post-upgrade state the values were – 1894.6 °C (flue gases) and 1182.9 °C (walls). In neither variant analysed does the maximum temperature of the walls exceed the ash softening temperature. Figs. 7-11 present a comparison between the temperature and velocity fields and the CO, O_2 and NO molar contents obtained from CFD modelling for the boiler in the reference and post-upgrade states.

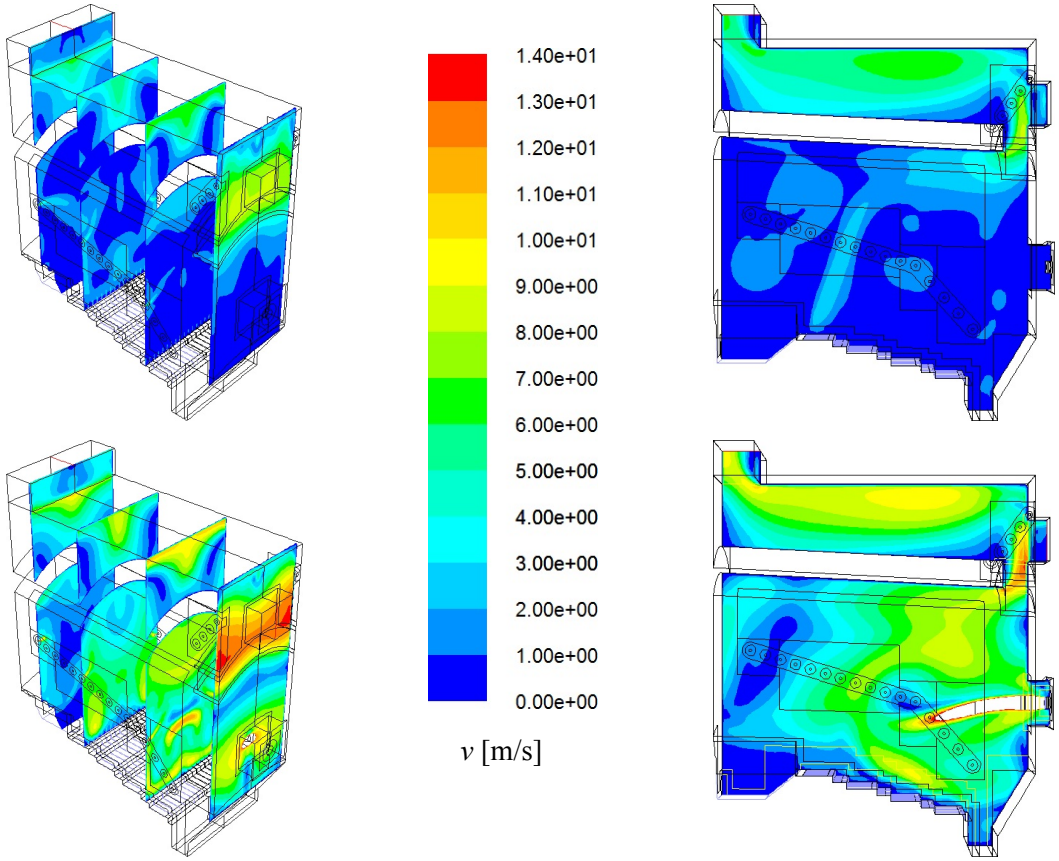

Fig. 7. Velocity fields for the boiler in the reference state (top) and in the post-upgrade state (bottom)

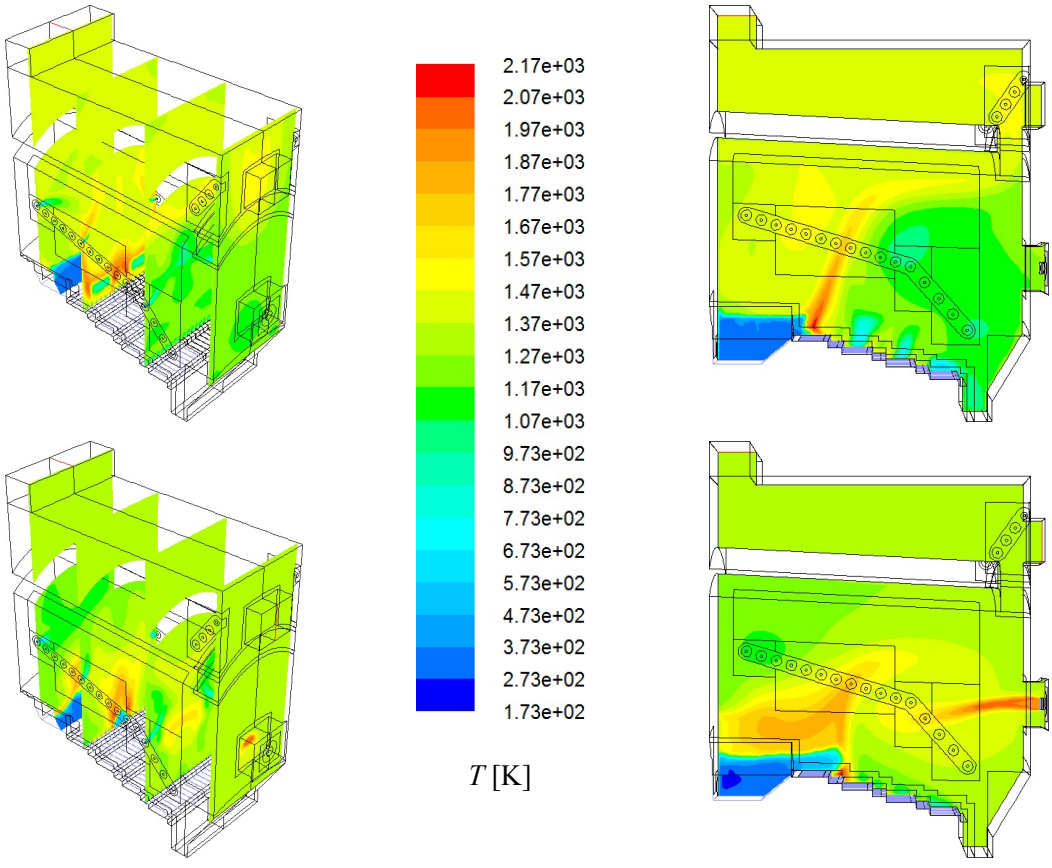

Fig. 8. Temperature fields for the boiler in the reference state (top) and in the post-upgrade state (bottom)

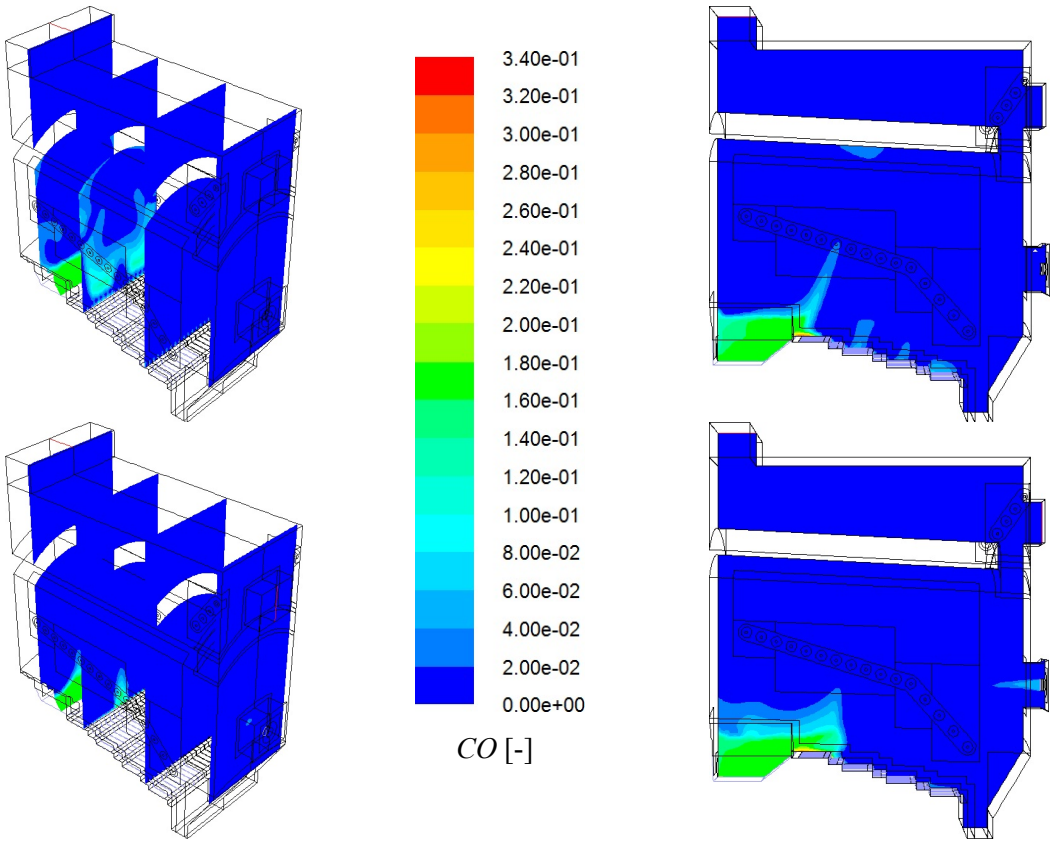

Fig. 9. CO molar content fields for the boiler in the reference state (top) and in the post-upgrade state (bottom)

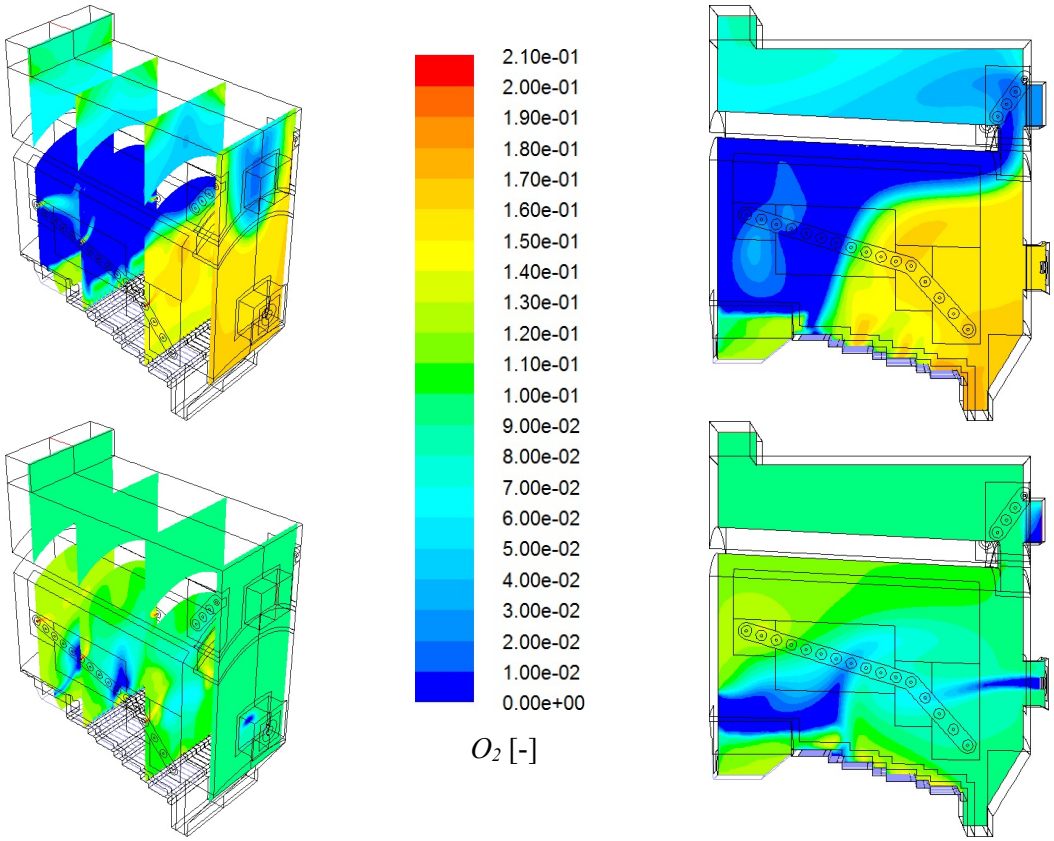

Fig. 10. O_2 molar content fields for the boiler in the reference state (top) and in the post-upgrade state (bottom)

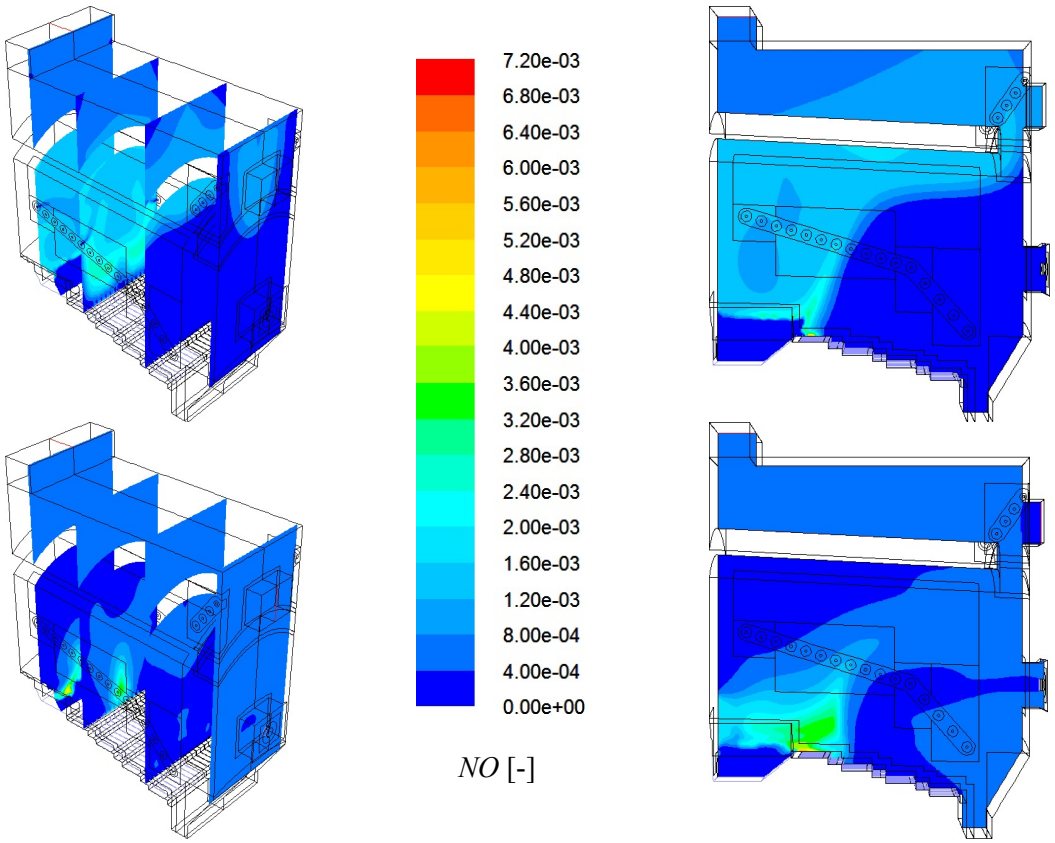

Fig. 11. NO molar content fields for the boiler in the reference state (top) and in the post-upgrade state (bottom)

5. DISCUSSION OF RESULTS

The results of modelling unequivocally point to the mode of the trough furnace operation with a distinctly marked area of intense combustion within the trough-grate interface, where the combustion of volatile fractions is accompanied by ignition of degassed fuel on the grate. The use of a jet blower system to shift flue gases into the gasifier and force combustible gas into the furnace chamber has a favourable effect on levelling the fields of velocity, temperature and concentrations. However, attention should be drawn to the fact that using air as the jet blower propellant involves the blower transformation into a kind of burner. Combustion takes place already within the jet blower – Fig. 6. Consequently, the jet blower structure and material are subject to additional thermal loads. Nevertheless, the function of the jet blower propellant may be very well fulfilled by compressed flue gases or water vapour – if available. A large volume of NOx emissions from wood combustion may probably be attributed to the high degree of conversion of nitrogen compounds contained in wood to NOx, which is caused by the smaller degree of wood coalification and the catalytic effect of calcium Ca (Mikulski, 1954). The amount of calcium oxides in biomass is bigger than that in fossil fuels (up to 50% by mass (Miles et al., 1995) compared to about 28% by mass in brown coal and about 8% by mass in hard coal (Zelena, 1963). Another reason for high NOx emissions is relatively small stoker furnace which is not conducive to primary reduction methods.

Nevertheless, the positive effect of co-combustion of gas from biomass gasification in the furnace chamber of the stoker-fired boiler is the substantial reduction in NO emissions by about 22%.

The work was co-financed by the National Centre for Research and Development (NCBiR) within the framework of the Technological Initiative II (IniTech), project No ZPB/57/65392/IT2/1 and by the National Science Centre (NCN) within project No. N N513 323640.

SYMBOLS

$A_{r,i}$	pre-exponential coefficient in the Arrhenius equation for *i*-th reaction
C_j	molar concentration of *j*-th reacting substance, kmol/m^3
C^m_j	mass concentration of *j*-th reacting substance, kg/m^3
D_i	diffusion coefficient for *i*-th reaction, m/s
$E_{r,i}$	activation energy in the Arrhenius equation for *i*-th reaction, J/kmol
k_i	constant rate of i-th reaction
(MR)	universal gas constant, J/(kmol K)
p	pressure, Pa
r_i	unit rate of *i*-th reaction, kmol/(m^3·s)
t	temperature, °C
T	temperature, K
v	velocity, m/s
$(_i)$	molar content of *i*-th substance, -

Subscripts

max	maximum
min	minimum
g	process gas
p	propelling air

REFERENCES

De Souza-Santos M.L., 1989. Comprehensive modelling and simulation of fluidized bed boilers and gasifiers. *Fuel*, 68, 1507-1521. DOI: 10.1016/0016-2361(89)90288-3.

Dryer F.L., Glassman I., 1973. High-temperature oxidation of CO and CH_4. *Symposium (International) on Combustion*, 14, 987-1003.

Fluent 6.3 User's Guide. Fluent Inc, 2006.

Hernik B., 2014. Numerical calculations of WR-40 boiler based on its zero-dimensional model. *Chem. Process Eng.*, 35, 173-180. DOI: 10.2478/cpe-2014-0013.

Kordylewski W. (Ed.), 2008. *Spalanie i paliwa*. Oficyna Wydawnicza Politechniki Wrocławskiej, Wrocław.

Litka R., Kalisz S., 2012. Thermochemical analysis of a flue gas-driven biomass gasification. *Chem. Process Eng.*, 33, 487-503. DOI: 10.2478/v10176-012-0041-y.

Mehrabian R., Zahirovic S., Scharler R., Obernberger I., Kleditzsch S., Wirtz S., Scherer V., Lu H., Baxter L.L., 2012. A CFD model for thermal conversion of thermally thick biomass particles. *Fuel Process. Technol.*, 95, 96-108. DOI: 10.1016/j.fuproc.2011.11.021.

Mikulski C., 1954. *Kotły parowe* (*wytwornice pary*). Państwowe Wydawnictwo Naukowe, Warszawa.

Miles T., Baxter L., Bryers R., Jenkins B., Oden L., 1995. Alkali deposits found in biomass power plants: A preliminary investigation of their extent and nature. *National Renewable Energy Laboratory*. Available at: http://www.nrel.gov/docs/legosti/fy96/8142v1.pdf.

Miltner M., Makaruk A., Harasek M., Friedl A., 2006. CFD-Modelling for the combustion of solid balled biomass. *Fifth International Conference on CFD in the Process Industries*, *CSIRO.* Melbourne, Australia.

Ostrowski Z., Zabłocki K., Zagórski J., Zmysłowski A., 1956. *Kotły parowe*, Vol. I. Państwowe Wydawnictwa Techniczne, Warszawa.

Patent PL 212497. *A method and a biomass pyrolysis installation before the co-combustion process, especially in power boilers*. Patent Office of the Republic of Poland (UPRP).

Pronobis M., Wojnar W., 2013. The impact of biomass co-combustion on the erosion of boiler convection surfaces. *Energy Convers. Manage.*, 74, 462-470. DOI: 10.1016/j.enconman.2013.06.059.

Smoot L.D., Smith P.J., 1985. *Coal combustion and gasification*. Plenum Press, New York.

Türschmid R., 1988. *Kotłownie i elektrociepłownie przemysłowe. Obliczenia z zakresu oszczędnej eksploatacji i modernizacji*. Arkady, Warszawa.

Patent PL 212557. *A method and a biomass carbonization and gasification installation before the co-combustion process, especially in power boilers*. Patent Office of the Republic of Poland (UPRP).

Patent PL 214645. *A method and a biomass gasification installation before the co-combustion process, especially in power boilers*. Patent Office of the Republic of Poland (UPRP).

Zelena S., 1963. *Obsługa kotłów parowych*. WNT Warszawa.

Received 11 March 2015
Received in revised form 29 December 2015
Accepted 12 January 2016